Journal of New Technology and Materials (JNTM)
J. New Technol. Mater.
Vol. 10, N°02 (2020)55-63

OEB Univ. Publish. Co.

Photodegradation of alachlor by H_2O_2/UV process in aqueous media: kinetic modeling

N. Djadi [a*] and W. Kaabar [a]

[a] *Département de Chimie, Faculté des Sciences Exactes, Université des Frères Mentouri Constantine, Algérie*

*Corresponding author, email: djadi.nabila@umc.edu.dz

Received date: Jan. 13, 2020 ; revised date: Nov. 02, 2020 ; accepted date: Nov. 04, 2020

Abstract

A kinetic model, which predicts Alachlor degradation by hydrogen peroxide-ultraviolet irradiation (H_2O_2/UV) process in synthetic and natural water matrices is developed, and validated with experimental results issued from the literature. The developed model is based on the elementary (photo)chemical reactions known to occur during the H_2O_2/UV process and their rate constants reported in the literature. The model does not employ the pseudo-steady-state assumption. It takes into account the pH decrease during the degradation and considers the presence of carbonate species and natural organic matter (NOM) in the system. Model verification was done by predicting Alachlor degradation under different process parameters: H_2O_2 concentration, solution pH and UV light intensity. Predicted results have shown good agreement with experimental data. Therefore, the model is considered to be valid and can be used for optimization purposes.

Keywords: kinetic model, H_2O_2/UV process; Alachlor; carbonate species; natural organic matter

1. Introduction

The use of pesticides brings great benefit to agriculture; they fight various organisms considered as harmful to the agricultural crops. However, their detection in air, water and soil is an issue of worldwide concern, since these chemicals can threaten the human health and affect the aquatic ecosystem, even at low concentrations [1].

Alachlor is an herbicide of the chloroacetanilide family, used for unwanted plants control in agricultural crops. This compound has been detected in groundwaters and surface waters [2–4]. It is known by its serious effect on human health owing to its endocrine disruptor action and carcinogenic activity [2,4–6]. Besides, it is toxic to many organisms that makes conventional biological processes inappropriate for its removal from water [2]. Therefore, an appropriate treatment of this compound is required. A promising solution to accomplish this goal lies in the use of advanced oxidation processes (AOPs).

AOPs are chemical treatment developed to remove toxic and persistent organic contaminants from water by oxidation. These processes generally employ various reagents such as oxidizing agents (hydrogen peroxide, persulfate, ozone, etc) and/or catalysts (semiconductors, metal salts, metal oxides, etc) along with energy sources (light sources, ultrasound waves, electrical energies, etc) to produce radicals, primarily but not exclusively hydroxyl radicals ($HO^{\bullet}$), known by their very high reactivity and non-selective nature [7]. AOPs could be applied for the purification of drinking water as well as for the remediation of polluted waters and wastewaters. They have been shown as promising processes for the degradation of pollutants belonging to various organic contaminant classessuch as pesticides, pharmaceuticals, organic industrial compounds, etc [8–10].

Hydrogen peroxide-ultraviolet irradiation (H_2O_2/UV) process is one of the most widely used AOPs, due to its advantages over other processes. The H_2O_2/UV process is characterized by its high degradation efficiency, relatively low operating cost and easy operation. Further, it can be applied at neutral pH. Moreover, no recovery or extraction of a catalyst is needed at the end of the process. Yet, the main factor that limit the process efficiency is the low molar absorption coefficient of H_2O_2 in the UV-C region (ε_{H2O2} = 18.6 M^{-1} cm^{-1} at 254 nm). To offset this disadvantage, a large amount of H_2O_2 is required to produce enough of $HO^{\bullet}$ radicals in the system. However, this leads to a second limitation, which is the scavenging effect of H_2O_2 when it is used at high concentrations. Further, the effectiveness of the process is restricted by the presence of UV absorbers and $HO^{\bullet}$ radicals scavengers, which reduce the efficiency of the process with respect to the pollutant of interest. Therefore, the optimization of the H_2O_2/UV process is required in order to avoid these limitations and take advantages from the process performances.

The focus of this study is to evaluate the performance of a kinetic model that predicts Alachlor degradation by H_2O_2/UV process, in the presence of carbonate species and natural organic matter (NOM), the most common constituents of natural waters. The performance of the kinetic model is evaluated by predicting Alachlor degradation under different process parameters; H_2O_2 concentration, solution pH and UV light intensity. The main goal is the use of the kinetic model for optimization purposes.

2. Methodology

2.1. Model development

2.1.1. Assumptions

The proposed model is formulated for predicting Alachlor degradation in the presence of carbonate species and NOM by H_2O_2/UV process in a completely mixed batch reactor (CMBR). The chemical structure and properties of Alachlor are described in Table 1. In this model, the kinetics of radical species are not described on the basis of the pseudo-steady-state assumption; the net formation rate of radical species is zero. The solution pH decrease during the degradation is included; the pH decrease is attributed to carbon dioxide formation. The degradation of Alachlor is considered to occur via direct photolysis and indirect decomposition by $HO^\bullet$ radicals; degradation by other reactive oxygen species ($HO_2^\bullet$, $O_2^{\bullet-}$ and $CO_3^{\bullet-}$ radicals) and organic radicals generated from NOM photolysis is neglected, since these radicals selectively react with organic compounds and reaction rate constants of these and other inorganic radicals are usually around two or three orders of magnitude smaller than those of $HO^\bullet$ radicals. While the $HO^\bullet$ radicals react nonselectively with different compounds in water with reaction rate constants that range from 10^6 to 10^{10} M^{-1} s^{-1}. It is supposed that there is no interaction of transformation products with UV irradiation and $HO^\bullet$ radicals since only trace levels of formaldehyde, acetaldehyde, glyoxal, glyoxylic acid and 2-chloroacetaldehyde were detected as transformation products [17]. Furthermore, it is assumed that there is no Alachlor decay by hydrolysis and direct reaction with H_2O_2. The considered UV light absorbing species in this system are organic compounds (Alachlor and NOM), hydrogen peroxide and its conjugate base (H_2O_2 and HO_2^-).

2.1.2. Kinetic rate expressions

Table 2 summarizes the elementary (photo)chemical reactions known to occur in the H_2O_2/UV process along with their literature reported rate constants.

The decomposition rate of Alachlor by direct photolysis (reaction 18 in Table 2) is described by Equation (1):

$$\frac{d[\text{Alachlor}]}{dt} = -\Phi_{\text{Alachlor}} f_{\text{Alachlor}} I_0 (1 - e^{-2.303A}) \qquad (1)$$

Where Φ_{Alachlor} (mol E^{-1}) represents the quantum yield of Alachlor at 254 nm, f_{Alachlor} the fraction of the UV irradiation absorbed by Alachlor, I_0 (E L^{-1} s^{-1}) the UV irradiation intensity of the lamp at 254 nm and A the total absorbance of the solution. f_{Alachlor} and A are denoted by Equations (2 and 3):

$$f_{Alachlor} = \frac{\varepsilon_{\text{Alachlor}} b[\text{Alachlor}]}{A} \qquad (2)$$

$$A = \varepsilon_{\text{Alachlor}} b[\text{Alachlor}] + \varepsilon_{\text{NOM}} b[\text{NOM}] + \varepsilon_{H_2O_2} b[H_2O_2] + \varepsilon_{HO_2^-} b[HO_2^-] \qquad (3)$$

Where $\varepsilon_{\text{Alachlor}}$, ε_{NOM}, ε_{H2O2} and ε_{HO2-} (M^{-1} cm^{-1}) represent the molar absorption coefficients of Alachlor, NOM, H_2O_2 and HO_2^-, respectively at 254 nm, b (cm) the effective optical pathlength of the photoreactor and [Alachlor], [NOM], $[H_2O_2]$ and $[HO_2^-]$ (M) the molar concentrations of Alachlor, NOM, H_2O_2 and HO_2^-, respectively. The reaction rates of other photolysis reactions are written in the same way.

The decomposition rate of Alachlor by $HO^\bullet$ radicals (reaction 19 in Table 2) is represented by Equation (4):

$$\frac{d[\text{Alachlor}]}{dt} = -k_{HO\bullet,\text{Alachlor}}[\text{Alachlor}][HO^\bullet] \qquad (4)$$

Where [Alachlor] and $[HO^\bullet]$ (M) represent the molar concentrations of Alachlor and $HO^\bullet$ radicals, respectively and $k_{HO\bullet,\text{Alachlor}}$ (M^{-1} s^{-1}) the second-order rate constant for the reaction between Alachlor and $HO^\bullet$ radicals. The reaction rates of other second-order reactions are written in the same manner.

The equilibrium reactions are treated just as the second-order reactions using forward and backward reaction rate constants.

The kinetic rate expressions of the chemical species listed in Table 2 are formulated as Equations (5 – 17):

$$\frac{d[\text{Alachlor}]}{dt} = -\Phi_{\text{Alachlor}} f_{\text{Alachlor}} I_0 (1 - e^{-2.303A}) - k_{HO\bullet,\text{Alachlor}}[HO^\bullet][\text{Alachlor}] \qquad (5)$$

$$\frac{d[H_2O_2]}{dt} = -\Phi_{H2O2} f_{H2O2} I_0 (1 - e^{-2.303A}) - k_2[H_2O_2][HO^\bullet] - k_4[H_2O_2][HO_2^\bullet] - k_5[H_2O_2][O_2^{\bullet-}] - k_8[H_2O_2][CO_3^{\bullet-}] + k_{10}[HO^\bullet][HO^\bullet] + k_{12}[HO_2^\bullet][HO_2^\bullet] - k_{for1}[H_2O_2] + k_{back1}[HO_2^-][H^+] \qquad (6)$$

$$\frac{d[HO_2^-]}{dt} = -\Phi_{HO2-} f_{HO2-} I_0 (1 - e^{-2.303A}) - k_3[HO_2^-][HO^\bullet] - k_9[HO_2^-][CO_3^{\bullet-}] + k_{13}[HO_2^\bullet][O_2^{\bullet-}] + k_{for1}[H_2O_2] - k_{back1}[HO_2^-][H^+] \qquad (7)$$

$$\begin{aligned}\frac{d[HO\cdot]}{dt} = &+ 2\,\Phi_{H2O2} f_{H2O2} I_0 (1 - e^{-2.303A}) + 2\,\Phi_{HO2-} f_{HO2-} I_0 (1 - e^{-2.303A}) \\ &- k_2[H_2O_2][HO^\bullet] - k_3[HO_2^-][HO^\bullet] + k_4[H_2O_2][HO_2^\bullet] \\ &+ k_5[H_2O_2][O_2^{\bullet-}] - k_6[HO^\bullet][CO_3^{2-}] - k_7[HO^\bullet][HCO_3^-] \\ &- 2\,k_{10}[HO^\bullet][HO^\bullet] - k_{11}[HO^\bullet][HO_2^\bullet] - k_{14}[HO^\bullet][O_2^{\bullet-}] \\ &- k_{15}[HO^\bullet][CO_3^{\bullet-}] - k_{HO\bullet,\text{Alachlor}}[HO^\bullet][\text{Alachlor}] \\ &- k_{HO\bullet,\text{NOM}}[\text{NOM}][HO^\bullet]\end{aligned} \qquad (8)$$

$$\frac{d[O_2^{\cdot-}]}{dt} = -k_5[O_2^{\bullet-}][H_2O_2] - k_{13}[HO_2^\bullet][O_2^{\bullet-}] - k_{14}[O_2^{\bullet-}][HO^\bullet] - k_{16}[O_2^{\bullet-}][CO_3^{\bullet-}] + k_{for2}[HO_2^\bullet] - k_{back2}[O_2^{\bullet-}][H^+] \qquad (9)$$

$$\frac{d[HO_2^{\cdot}]}{dt} = +k_2[H_2O_2][HO^\bullet] + k_3[HO_2^-][HO^\bullet] - k_4[HO_2^\bullet][H_2O_2] + k_8[H_2O_2][CO_3^{\bullet-}] + k_9[CO_3^{\bullet-}][HO_2^-] - k_{11}[HO_2^\bullet][HO^\bullet] - 2\,k_{12}[HO_2^\bullet][HO_2^\bullet] - k_{13}[HO_2^\bullet][O_2^{\bullet-}] - k_{for2}[HO_2^\bullet] + k_{back2}[O_2^{\bullet-}][H^+] \qquad (10)$$

$$\frac{d[H_2CO_3^*]}{dt} = -k_{for3}[H_2CO_3^*] + k_{back3}[HCO_3^-][H^+] \qquad (11)$$

$$\frac{d[HCO_3^-]}{dt} = -k_7[HCO_3^-][HO^\bullet] + k_8[CO_3^{\bullet-}][H_2O_2] + k_{for3}[H_2CO_3^*] - k_{back3}[HCO_3^-][H^+] - k_{for4}[HCO_3^-] + k_{back4}[CO_3^{2-}][H^+] \qquad (12)$$

$$\frac{d[CO_3^{2-}]}{dt} = -k_6[HO^\bullet][CO_3^{2-}] + k_9[CO_3^{\bullet-}][HO_2^-] + k_{16}[CO_3^{\bullet-}][O_2^{\bullet-}] + k_{for4}[HCO_3^-] - k_{back4}[CO_3^{2-}][H^+] \qquad (13)$$

$$\frac{d[CO_3^{-}]}{dt} = + k_6[HO^\bullet][CO_3^{2-}] + k_7[HO^\bullet][HCO_3^-] - k_8[CO_3^{\bullet-}][H_2O_2] - k_9[CO_3^{\bullet-}][HO_2^-] - k_{15}[CO_3^{\bullet-}][HO^\bullet] - k_{16}[CO_3^{\bullet-}][O_2^{\bullet-}] - 2\,k_{17}[CO_3^{\bullet-}][CO_3^{\bullet-}] \qquad (14)$$

$$\frac{d[H^+]}{dt} = + k_{for1}[H_2O_2] - k_{back1}[HO_2^-][H^+] + k_{for2}[HO_2^\bullet] - k_{back2}[O_2^{\bullet-}][H^+] + k_{for3}[H_2CO_3^*] - k_{back3}[HCO_3^-][H^+] + k_{for4}[HCO_3^-] - k_{back4}[CO_3^{2-}][H^+] \qquad (15)$$

Table 1: Chemical structure and properties of Alachlor

Chemical structure	Chemical properties
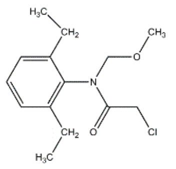	CAS: 15972-60-8 Molecular formula: $C_{14}H_{20}ClNO_2$ Molecular weight: 269.77 g mol^{-1} Water solubility: 240 mg L^{-1}
Data source: https://chem.nlm.nih.gov/chemidplus/.	

Table 2: Reaction scheme used in the kinetic model

No	Reactions	Rate constants	References
1	$H_2O_2 \xrightarrow{h\nu} 2\,HO^\bullet$ $HO_2^- + H_2O \xrightarrow{h\nu} 2\,HO^\bullet + OH^-$	$\varepsilon_{H2O2} = 18.6\ M^{-1}cm^{-1}$, $\Phi_{H2O2} = 0.5$ mol E^{-1} $\varepsilon_{HO2-} = 228\ M^{-1}cm^{-1}$, $\Phi_{HO2-} = 0.5$ mol E^{-1}	[18] [19]
2	$HO^\bullet + H_2O_2 \rightarrow HO_2^\bullet + H_2O$	$k_2 = 2.7 \times 10^7\ M^{-1}\ s^{-1}$	[20]
3	$HO^\bullet + HO_2^- \rightarrow HO_2^\bullet + OH^-$	$k_3 = 7.5 \times 10^9\ M^{-1}\ s^{-1}$	[21]
4	$HO_2^\bullet + H_2O_2 \rightarrow HO^\bullet + H_2O + O_2$	$k_4 = 3\ M^{-1}\ s^{-1}$	[22]
5	$O_2^{\bullet-} + H_2O_2 \rightarrow HO^\bullet + O_2 + OH^-$	$k_5 = 0.13\ M^{-1}\ s^{-1}$	[23]
6	$HO^\bullet + CO_3^{2-} \rightarrow CO_3^{\bullet-} + OH^-$	$k_6 = 3.9 \times 10^8\ M^{-1}\ s^{-1}$	[20]
7	$HO^\bullet + HCO_3^- \rightarrow CO_3^{\bullet-} + H_2O$	$k_7 = 8.5 \times 10^6\ M^{-1}\ s^{-1}$	[20]
8	$CO_3^{\bullet-} + H_2O_2 \rightarrow HO_2^\bullet + HCO_3^-$	$k_8 = 8 \times 10^5\ M^{-1}\ s^{-1}$	[24]
9	$CO_3^{\bullet-} + HO_2^- \rightarrow HO_2^\bullet + CO_3^{2-}$	$k_9 = 3 \times 10^7\ M^{-1}\ s^{-1}$	[25]
10	$HO^\bullet + HO^\bullet \rightarrow H_2O_2$	$k_{10} = 5.5 \times 10^9\ M^{-1}\ s^{-1}$	[20]
11	$HO^\bullet + HO_2^\bullet \rightarrow H_2O + O_2$	$k_{11} = 6.6 \times 10^9\ M^{-1}\ s^{-1}$	[26]
12	$HO_2^\bullet + HO_2^\bullet \rightarrow H_2O_2 + O_2$	$k_{12} = 8.3 \times 10^5\ M^{-1}\ s^{-1}$	[27]
13	$HO_2^\bullet + O_2^{\bullet-} \rightarrow HO_2^- + O_2$	$k_{13} = 9.7 \times 10^7\ M^{-1}\ s^{-1}$	[27]
14	$HO^\bullet + O_2^{\bullet-} \rightarrow O_2 + OH^-$	$k_{14} = 7 \times 10^9\ M^{-1}\ s^{-1}$	[28]
15	$HO^\bullet + CO_3^{\bullet-} \rightarrow$ products	$k_{15} = 3 \times 10^9\ M^{-1}\ s^{-1}$	[29]
16	$CO_3^{\bullet-} + O_2^{\bullet-} \rightarrow CO_3^{2-} + O_2$	$k_{16} = 6.5 \times 10^8\ M^{-1}\ s^{-1}$	[24]
17	$CO_3^{\bullet-} + CO_3^{\bullet-} \rightarrow$ products	$k_{17} = 3 \times 10^7\ M^{-1}\ s^{-1}$	[30]
18	Alachlor $\xrightarrow{h\nu}$ products	$\varepsilon_{Alachlor} = 466.7\ M^{-1}cm^{-1}$, $\Phi_{Alachlor} = 0.14$ mol E^{-1}	[17]
19	$HO^\bullet$ + Alachlor $\rightarrow$ products	$k_{HO\bullet,NOM} = 1.2 \times 10^8\ M^{-1}\ s^{-1}$	[17]
20	NOM $\xrightarrow{h\nu}$ products	$\varepsilon_{NOM} = 18000\ M^{-1}cm^{-1}$; $\Phi_{NOM} = 1.9 \times 10^{-5}$ mol E^{-1}	[17]
21	$HO^\bullet$ + NOM $\rightarrow$ products	$k_{HO\bullet,NOM} = 1.2 \times 10^8\ M^{-1}\ s^{-1}$	[17]
22	$H_2O_2 \Leftrightarrow H^+ + HO_2^-$, $pKa_1 = 11.6$	$k_{for1} = 2.51 \times 10^{-2} M^{-1}\ s^{-1}$, $k_{back1} = 10^{10} s^{-1}$	[31]
23	$HO_2^\bullet \Leftrightarrow H^+ + O_2^{\bullet-}$, $pKa_2 = 4.86$	$k_{for2} = 1.58 \times 10^5 M^{-1}\ s^{-1}$, $k_{back2} = 10^{10} s^{-1}$	[31]
24	$H_2CO_3^* \Leftrightarrow H^+ + HCO_3^-$, $pKa_3 = 6.3$	$k_{for3} = 4.5 \times 10^3 M^{-1}\ s^{-1}$, $k_{back3} = 10^{10} s^{-1}$	[31]
25	$HCO_3^- \Leftrightarrow H^+ + CO_3^{2-}$, $pKa_4 = 10.36$	$k_{for4} = 4.5 \times 10^{-1} M^{-1}\ s^{-1}$, $k_{back4} = 10^{10} s^{-1}$	[31]

$$\frac{d[HO^-]}{dt} = +\ \Phi_{HO2-}f_{HO2-}I_0(1-e^{-2.303A}) + k_3[HO_2^-][HO^\bullet] + k_5[H_2O_2][O_2^{\bullet-}] + k_6[CO_3^{2-}][HO^\bullet] + k_{14}[O_2^{\bullet-}][HO^\bullet] \quad (16)$$

$$\frac{d[NOM]}{dt} = -\ \Phi_{NOM}f_{NOM}I_0(1-e^{-2.303A}) - k_{HO\bullet,NOM}[NOM][HO^\bullet] \quad (17)$$

In the kinetic rate expressions described above, plus and minus signs indicate the production and consumption of species, respectively.

2.1.3. Initial conditions

The following initial conditions are considered: the initial concentrations of the organic compounds (Alachlor and NOM) are imposed, while those of radicals are taken as zero. The initial concentration of H+ is set according to the initial solution pH. For equilibrium species (H_2O_2/HO_2^-, $H_2CO_3^*/HCO_3^-$ and HCO_3^-/CO_3^{2-}), the initial concentrations of the individual species are calculated using the total concentration, the initial solution pH and the equilibrium constant, as shown in Equations (18 – 22). Furthermore, the rate constants of the elementary chemical reactions known to occur during the UV/H_2O_2 process, the photochemical constants of the organic compounds (Ɛ, Φ and $k_{HO\bullet}$), H_2O_2 and HO_2^- (Ɛ and Φ) as well as the characteristics of the UV system (I_0 and b) are used as inputs.

$$[H_2O_2]_{ini} = \frac{[H_2O_2]_{tot}}{(1+10^{-pKa1+pH})} \quad (18)$$

$$[HO_2^-]_{ini} = \frac{[H_2O_2]_{tot}}{(1+10^{-pH+pKa1})} \quad (19)$$

$$[HCO_3^-]_{ini} = \frac{[C_{T,CO3}]_{tot}}{1+10^{-pH+pKa3}+10^{-pKa4+pH}} \quad (20)$$

$$[H_2CO_3^*]_{ini} = [HCO_3^-]10^{-pH+pKa3} \quad (21)$$

$$[CO_3^{2-}]_{ini} = [HCO_3^-]10^{-pKa4+pH} \quad (22)$$

2.1.4. Numerical solution

The numerical solution of the stiff system of ordinary differential equations (ODE) is obtained by Matlab 2017 software using ODE15s function with relative and absolute tolerances of 10^{-8} and 10^{-10}, respectively.

2.2. Model validation

The experimental data obtained by Song and their co-workers [17] from the study of Alachlor degradation by H_2O_2/UV process were used to validate the developed model. In their laboratory study, the degradation of Alachlor was conducted in two separate series of experiments, where a synthetic solution that contains appropriate amount of sodium bicarbonate or a groundwater containing known concentrations of carbonate species and NOM were used. The H_2O_2/UV degradation of Alachlor was produced in a CMBR operating at constant temperature (25 °C). The UV irradiation was provided by a low-pressure mercury lamp that emits, primarily, monochromatic light at 254 nm. The characteristics of the UV system and the photochemical constants of the organic compounds were determined. The water quality was also evaluated. The values and determination methods are given in Table 3.

To compare the predicted results from the proposed model with the experimental ones, experimental data points were extracted from the experimental curves using the digitizing software Grafula 3. Then, the relative error (RE) has been quantified, according to Equation (23), in order to test the reliability of the proposed model.

$$RE\ (\%) = \frac{|k_{t\,pre} - k_{t\,exp}|}{k_{t\,exp}} \times 100 \quad (23)$$

Where $k_{t\ pre}$ and $k_{t\ exp}$ (s^{-1}) represent predicted and experimental time-based rate constants, respectively.

Table 3 : Input parameters for the kinetic model [17]

Parameters	Values	Determination method
UV system parameters	$I_0 = 1.8 / 2.4 \times 10^{-6}$ E L^{-1} s^{-1}	Actinometric measurement
	b = 5.1 cm	Actinometric measurement
Organic compound parameters	$Ɛ_{Alachlor} = 466.7\ M^{-1} cm^{-1}$	Spectrometric measurement
	$\Phi_{Alachlor} = 0.14$ mol E^{-1}	Actinometric measurement
	$k_{HO\bullet,Alachlor} = 2.2 \times 10^9\ M^{-1}\ s^{-1}$	Competitive kinetic experiment
	$Ɛ_{NOM} = 18000\ M^{-1} cm^{-1}$	Spectrometric measurement
	$\Phi_{NOM} = 1.9 \times 10^{-5}$ mol E^{-1}	Actinometric measurement
	$k_{HO\bullet,NOM} = 1.2 \times 10^8\ M^{-1}\ s^{-1}$	Competitive kinetic experiment
Water quality parameters	$[C_{T,CO3}]_0 = 3$ mM	Titrimetric method
	$[NOM]_0 = 10.6$ µM	UV-visible spectrometry

3. Results and discussion

3.1. Model prediction of Alachlor degradation

The prediction of Alachlor degradation by H_2O_2/UV process in synthetic and natural water matrices was made through Equations (5 – 16) and (5 – 17), respectively. Predicted and experimental results are illustrated in Figure 1. The obtained results show that the developed model predicted accurately the degradation of Alachlor in the presence of carbonate species and NOM under the studied conditions. However, in order to evaluate the performance of the kinetic model, further predictions under different process parameters should be examined.

The degradation of Alachlor by H_2O_2/UV process was found to follow the pseudo-first-order kinetics. In what follows, the pseudo-first order rate constants are used to compare predicted and experimental results.

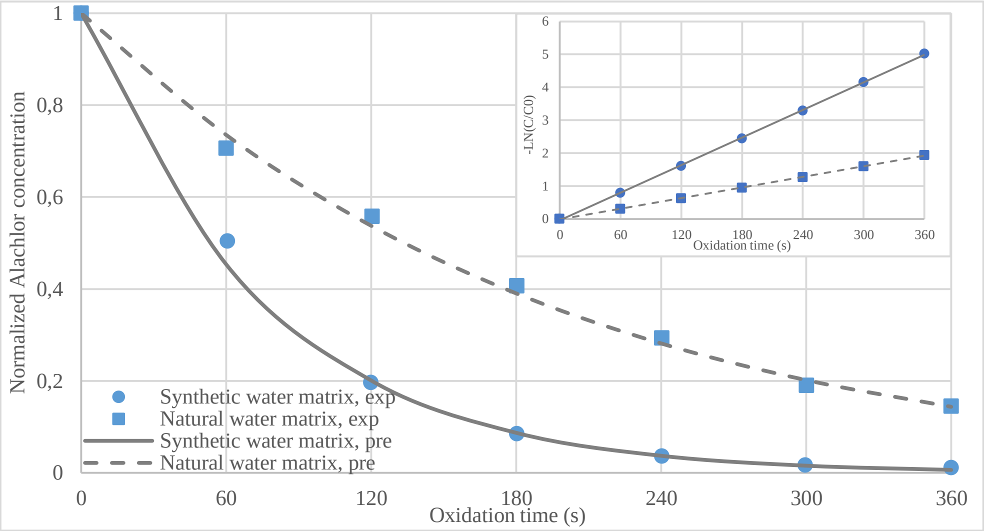

Figure 1. Comparison between experimental and predicted results for Alachlor degradation by H_2O_2/UV process
Synthetic water matrix: $[Alachlor]_0 = 1.7\ \mu M$, $[H_2O_2]_0 = 2\ mM$, pH = 8.3, $[C_{T,CO3}]_0 = 3\ mM$
Natural water matrix: $[Alachlor]_0 = 1.7\ \mu M$, $[H_2O_2]_0 = 2\ mM$, pH = 8.3, $[C_{T,CO3}]_0 = 3\ mM$, $[NOM]_0 = 10.6\ \mu M$
Inset: linear plot of Alachlor degradation

3.2. Effect of initial H_2O_2 concentration

The effect of initial H_2O_2 concentration on the degradation of Alachlor in synthetic and natural water matrices was investigated with H_2O_2 concentrations varying from 0.6 to 9 mM. The predicted and experimental rate constants of Alachlor degradation at different initial H_2O_2 concentrations are presented in Figure 2 and Table 4 (Group I). Results show that increasing the initial H_2O_2 concentration increases the Alachlor degradation rate up to initial concentrations of 3 and 4 mM for synthetic and natural water matrices, respectively. Beyond these concentrations the Alachlor degradation rates decrease. Initially, the enhancement of the degradation efficiency is attributed to the increased production of $HO^\bullet$ radicals from the photolysis of H_2O_2 until reaching an optimal H_2O_2 dosage. While, the reduction of the degradation efficiency is explained by the consumption of $HO^\bullet$ radicals by H_2O_2 beyond the optimal dosage (the second order rate constant of reaction 2 in Table 2). As expected, the degradation of Alachlor in the natural water matrix containing carbonate species and NOM decreases significantly as compared to the degradation in the synthetic water matrix that contains only carbonates species, due to the additional UV absorption and $HO^\bullet$ radicals scavenging effects of NOM. The model predicts well the experimental results, except for low (0.6 mM) and high (9 mM) initial H_2O_2 concentrations where an over prediction of the experimental data was obtained for both matrices. At low initial H_2O_2 concentration the direct photolysis of Alachlor becomes a relatively significant degradation pathway, the discrepancy under this condition is probably due to an inaccurate estimation of $\varepsilon_{Alachlor}$ and/or $\Phi_{Alachlor}$. However, the disagreement between predicted and experimental results at high initial H_2O_2 concentration could be attributed to an imprecise description of the inhibitory effect of H_2O_2 at high levels by the model.

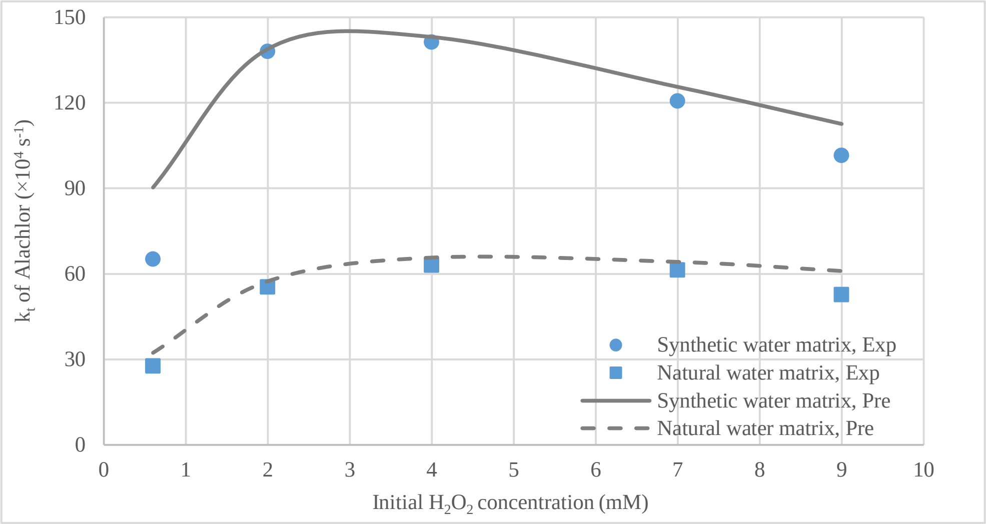

Figure 2. Experimental data and model profiles for the Alachlor degradation rate constant as a function of initial H_2O_2 concentration

Table 4: Comparison of predicted and experimental rate constants of Alachlor degradation, initial H_2O_2 concentration effect

$[Alachlor]_0$ (µM)	I_0 ($\times 10^6$ E L^{-1} s^{-1})	$[H_2O_2]_0$ (mM)	pH	$[C_{T,CO3}]_0$ (mM)	$[NOM]_0$ (µM)	$k_{t\ exp}$ ($\times 10^4$ s^{-1})	$k_{t\ pre}$ ($\times 10^4$ s^{-1})	RE (%)
Group I : change in $[H_2O_2]_0$								
1.7	1.8	0.6	8.3	3	0	65.2	90.3	38.5
1.7	1.8	2	8.3	3	0	138	138.9	0.65
1.7	1.8	4	8.3	3	0	141.3	143.1	1.3
1.7	1.8	7	8.3	3	0	120.7	125.6	4
1.7	1.8	9	8.3	3	0	101.6	112.6	10.8
1.7	1.8	0.6	8.3	3	10.6	27.7	32.3	16.6
1.7	1.8	2	8.3	3	10.6	55.4	57.4	3.6
1.7	1.8	4	8.3	3	10.6	63	65.7	4.3
1.7	1.8	7	8.3	3	10.6	61.4	64.2	4.6
1.7	1.8	9	8.3	3	10.6	52.7	61	15.7
1.7	2.4	2	8.3	3	10.6	79.7	76.2	4.4
1.7	2.4	4	8.3	3	10.6	89.5	86.9	2.9
1.7	2.4	7	8.3	3	10.6	81.5	84.9	4.2
1.7	2.4	9	8.3	3	10.6	77.3	81	4.8

3.3. Effect of initial solution pH

The effect of initial solution pH on the degradation of Alachlor in synthetic and natural water matrices was studied in the pH range of 6.1 – 8.6. Figure 3 and Table 5 (Group II) present the predicted and experimental rate constants of Alachlor degradation at various pH levels. Results indicate that, as the pH was increased from 6.1 to 8.6, there was a decrease in the Alachlor degradation rates. The reduction of the degradation efficiency is explained by the increase of HO_2^- and CO_3^{2-} concentrations with the increasing of pH. The increase in the concentrations of these two species reduces the degradation efficiency, as HO_2^- reacts with $HO^\bullet$ radicals faster than does H_2O_2 (thesecond order rate constants of reactions 2 and 3 in Table 2) and CO_3^{2-} is a strong scavenger of $HO^\bullet$ radicals compared to HCO_3^- (the second order rate constants of reactions 6 and 7 in Table 2). Evidently, the presence of the NOM in natural water matrix resulted in lower reaction kinetics as compared to the synthetic water matrix. An excellent agreement was found between predicted and experimental results in synthetic water matrix case. Alachlor degradation in natural water matrix was also satisfactorily predicted by the kinetic model, except at low pH level (pH = 6.1), where the model prediction manifested an over prediction of the experimental result. A plausible explanation could be the variation in NOM reactivity with $HO^\bullet$ radicals as a function of pH.

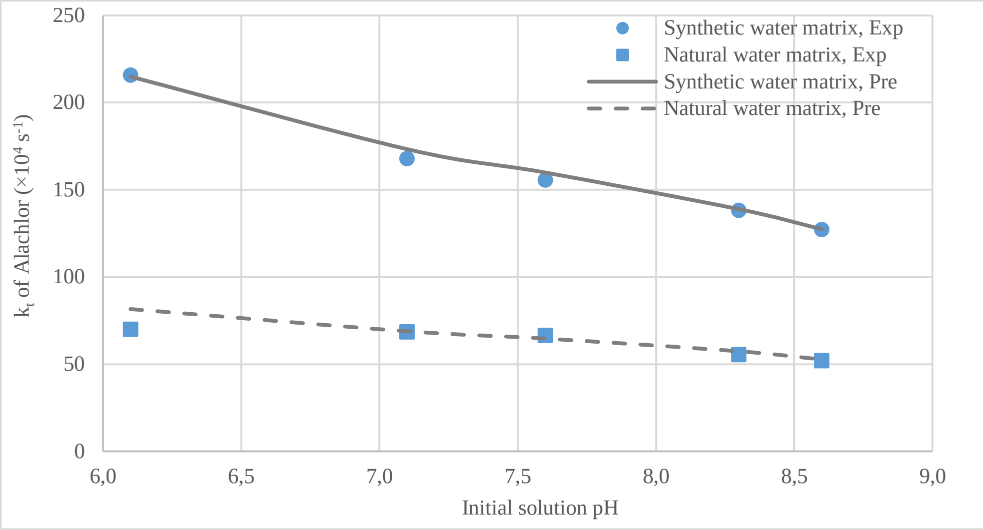

Figure 3. Experimental data and model profiles for Alachlor degradation rate constants as a function of initial solution pH

Table 5: Comparison of predicted and experimental rate constants of Alachlor degradation, initial solution pH effect

$[Alachlor]_0$ (µM)	I_0 ($\times 10^6$ E L^{-1} s^{-1})	$[H_2O_2]_0$ (mM)	pH	$[C_{T,CO3}]_0$ (mM)	$[NOM]_0$ (µM)	$k_{t\ exp}$ ($\times 10^4$ s^{-1})	$k_{t\ pre}$ ($\times 10^4$ s^{-1})	RE (%)
Group II : change in pH								
1.7	1.8	2	6.1	3	0	215.5	214.9	0.3
1.7	1.8	2	7.1	3	0	167.8	173.3	3.2
1.7	1.8	2	7.6	3	0	155.4	159.9	2.9
1.7	1.8	2	8.3	3	0	138	138.9	0.65
1.7	1.8	2	8.6	3	0	127.1	127.4	0.2
1.7	1.8	2	6.1	3	10.6	69.8	81.6	16.9
1.7	1.8	2	7.1	3	10.6	68.4	68.9	0.7
1.7	1.8	2	7.6	3	10.6	66.3	64.7	2.4
1.7	1.8	2	8.3	3	10.6	55.4	57.4	3.6
1.7	1.8	2	8.6	3	10.6	51.8	52.7	1.7

3.4. Effect of UV light intensity

The effect of UV light intensity on the degradation of Alachlor in natural water matrix was performed at two irradiation levels: 1.8 × 10^{-6} and 2.4 × 10^{-6} E L^{-1} s^{-1} and under different initial H_2O_2 concentrations: 0.6 – 9 mM. Figure 4 and Table 6 (Group III) present the predicted and experimental rate constants of Alachlor degradation at tested UV light intensities. Results show that increasing the UV light intensity increases the Alachlor degradation rates. The enhancement of the degradation efficiency is explained by the formation of a high amount of $HO^{\bullet}$ radicals at higher UV light intensity. Agreement between predicted and experimental results was well except for low and high initial H_2O_2 concentrations. The reasons of these discrepancies were previously explained in the effect of initial H_2O_2 concentration section.

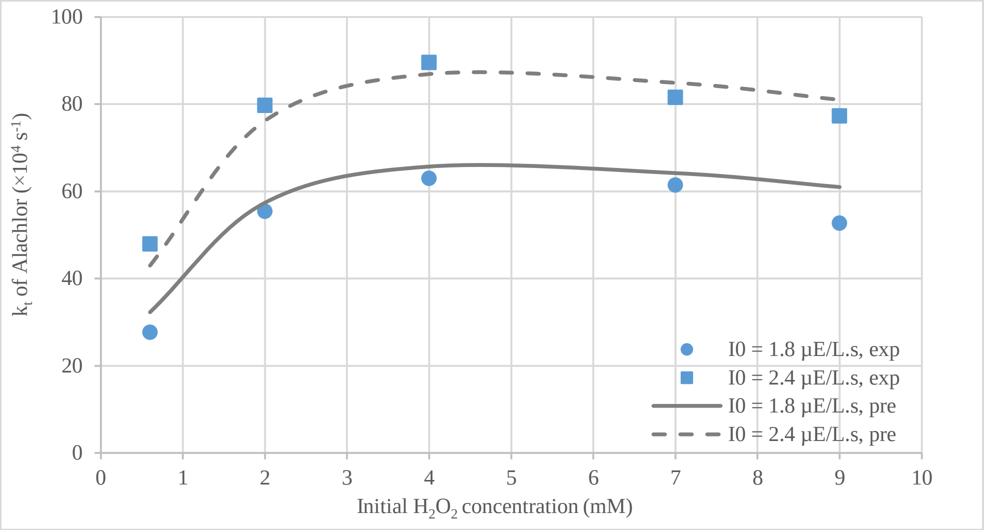

Figure 4. Experimental data and model profiles for the Alachlor degradation rate constant as a function of UV light

Table 6: Comparison of predicted and experimental rate constants of Alachlor degradation, UV light effect

$[Alachlor]_0$ (µM)	I_0 (× 10^6 E L^{-1} s^{-1})	$[H_2O_2]_0$ (mM)	pH	$[C_{T,CO3}]_0$ (mM)	$[NOM]_0$ (µM)	$k_{t\ exp}$ (× 10^4 s^{-1})	$k_{t\ pre}$ (× 10^4 s^{-1})	RE (%)
Group III : change in I_0								
1.7	1.8	0.6	8.3	3	10.6	27.7	32.3	16.6
1.7	1.8	2	8.3	3	10.6	55.4	57.4	3.6
1.7	1.8	4	8.3	3	10.6	63	65.7	4.3
1.7	1.8	7	8.3	3	10.6	61.4	64.2	4.6
1.7	1.8	9	8.3	3	10.6	52.7	61	15.7
1.7	2.4	0.6	8.3	3	10.6	47.9	43	10.2
1.7	2.4	2	8.3	3	10.6	79.7	76.2	4.4
1.7	2.4	4	8.3	3	10.6	89.5	86.9	2.9
1.7	2.4	7	8.3	3	10.6	81.5	84.9	4.2
1.7	2.4	9	8.3	3	10.6	77.3	81	4.8

4. Conclusion

In this study, a kinetic model based on the elementary (photo)chemical reactions known to occur during the H_2O_2/UV process and their rate constants reported in the literature was applied for the prediction of Alachlor degradation in the presence of carbonate species and NOM and under different process parameters. Based on the obtained results from this research, the developed model is shown to be able to accurately predict the following:

- The optimal H_2O_2 concentration for Alachlor degradation and the scavenging effect of H_2O_2 at concentrations above the optimal value. However, the model encounters difficulties for predicting Alachlor degradation at high initial H_2O_2 concentrations.
- The pH effect at varying levels. The obtained results highlight the importance of incorporating the pH dependence of second order rate constants of organic compounds in kinetic models.
- The UV light effect at different intensities.

References

[1] R. P. Schwarzenbach, T. Egli, T.B. Hofstetter, U. von Gunten, B. Wehrli, Annu. Rev. Environ. Resour. 35 (2010) 109–136.

[2] Y. K. Chang, Y.S. Wu, C.-S. Lu, P.-F. Lin, T.-Y. Wu, Water. Air. Soil Pollut. 226 (2015).

[3] S. Chiron, D. Barceló, J. Abian, M. Ferrer, F. Sanchez-Baeza, A. Messeguer, Environ. Toxicol. Chem. 14 (1995) 1287–1298.

[4] H. Katsumata, S. Kaneco, T. Suzuki, K. Ohta, Y. Yobiko, J. Photochem. Photobiol. Chem. 180 (2006) 38–45.

[5] M. -S. Kim, C.S. Ryu, B. W. Kim, Water Res. 39 (2005) 525–532.

[6] C. S. Ryu, M.-S. Kim, B. W. Kim, Chemosphere 53 (2003) 765–771.

[7] M. Mohajerani, M. Mehrvar, F. Ein-Mozaffari, Ind. Eng. Chem. Res. 49 (2010) 5367–5382.

[8] D. Juretic, H. Kusic, D.D. Dionysiou, B. Rasulev, A. Loncaric Bozic, Chem. Eng. J. 257 (2014) 229–241.

[9] E. Kowalska, M. Janczarek, J. Hupka, M. Grynkiewicz, Water Sci. Technol. 49 (2004) 261–266.

[10] B. A. Wols, C.H.M. Hofman-Caris, D.J.H. Harmsen, E.F. Beerendonk, Water Res. 47 (2013) 5876–5888.

[11] S. Dominguez, M.J. Rivero, P. Gomez, R. Ibañez, I. Ortiz, J. Ind. Eng. Chem. 37 (2016) 237–242.

[12] H. Kusic, N. Koprivanac, S. Horvat, S. Bakija, A.L. Bozic, Chem. Eng. J. 155 (2009) 144–154.

[13] C. Luo, J. Ma, J. Jiang, Y. Liu, Y. Song, Y. Yang, Y. Guan, D. Wu, Water Res. 80 (2015) 99–108.

[14] S. Luo, Z. Wei, R. Spinney, Z. Zhang, D.D. Dionysiou, L. Gao, L. Chai, D. Wang, R. Xiao, J. Hazard. Mater. 343 (2018) 132–139.

[15] L. Qin, Y. L. Lin, B. Xu, C.-Y. Hu, F. X. Tian, T.-Y. Zhang, W. Q. Zhu, H. Huang, N. Y. Gao, Water Res. 65 (2014) 271–281.

[16] D. Spasiano, R. Marotta, I. Gargano, I.D. Somma, G. Vitiello, G. D'Errico, R. Andreozzi, Chem. Eng. J. 249 (2014) 130–142.

[17] W. Song, V. Ravindran, M. Pirbazari, Chem. Eng. Sci. 63 (2008) 3249–3270.

[18] D. H. Volman, J.C. Chen, J. Am. Chem. Soc. 81 (16) (1959) 4141–4144.

[19] J. H. Baxendale, J.A. Wilson, Trans. Faraday Soc. 53 344 (1957).

[20] G.V. Buxton, C.L. Greenstock, W.P. Helman, A.B. Ross, J. Phys. Chem. 17 (1988) 513–886.

[21] H. Christensen, K. Sehested, H. Corfitzen, J. Phys. Chem. 86 (1982) 1588–1590.

[22] W. H. Koppenol, J. Butler, J.W. van Leeuwen, Photochem. Photobiol. 28 (1978) 655–658.

[23] J. Weinstein, B.H.J. Bielski, J. Am. Chem. Soc. (1979) 58–62.

[24] P. Neta, R.E. Huie, J. Phys. Chem., 17 (1988) 1027–1284.

[25] Z. D. Draganić, A. Negrón-Mendoza, K. Sehested, S.I. Vujošević, R. Navarro-Gonzáles, M.G. Albarrán-Sanchez, I.G. Draganić, Int. J. Radiat. Appl. Instrum. Part C Radiat. Phys. Chem. 38 (1991) 317–321.

[26] F. Beck, Int. J. Radiat. Phys. Chem. 1 (3) (1969) 361–371.

[27] B. Bielski, D. Cabelli, R. Arudi, A. Ross, J. Phys. Chem. 14 (4) (1985) 1041–1100.

[28] J. Holeman, E. Bjergbakke, K. Sehested, Proceeding of the Tihany Symposium on Radiation Chemistry. 6 (1) (1987) 149–153.

[29] K. Sehested, O.L. Rasmussen, H. Fricke, J. Phys. Chem. 72 (2) (1968) 626–631.

[30] R. E. Huie, C.L. Clifton, J. Phys. Chem. 94 (1990) 8561–8567.

[31] B. A. Wols, D.J.H. Harmsen, J. Wanders-Dijk, E.F. Beerendonk, C.H.M. Hofman-Caris, Water Res. 75 (2015) 11–24.